福昕PDF编辑器

• 永久　• 轻巧　• 自由

升级会员　　批量购买

永久使用

无限制使用次数

极速轻巧

超低资源占用，告别卡顿慢

自由编辑

享受Word一样的编辑自由

扫一扫，关注公众号

Infrared Small Target Detection Based on Multiscale Local Contrast Measure Using Local Energy Factor

Chaoqun Xia, Xiaorun Li, Liaoying Zhao, and Rui Shu

***Abstract*— Infrared small target detection is one of the most important parts of infrared search and tracking (IRST) system. Generally, the small and dim target is of low signal-to-noise ratio and buried in the complicated background and heavy noise, which makes it extremely difficult to be detected with low false alarm rates. To solve this problem, we propose a small target detection method based on multiscale local contrast measure. Different from conventional methods, we novelly measure the local contrast from two aspects: local dissimilarity and local brightness difference. First, we present a new dissimilarity measure called the local energy factor (LEF) to describe the dissimilarity between the small targets and their surrounding backgrounds. Second, the feature of the brightness difference between the small targets and the backgrounds is utilized. Afterward, the local contrast is measured by taking both features of the above into account. Finally, an adaptive segmentation method is applied to extract the small targets from the backgrounds. Extensive experiments on real test data set demonstrate that our approach outperforms the state-of-the-art approaches.**

***Index Terms*— Infrared small target detection, local dissimilarity measure, multiscale local contrast measure.**

I. Introduction

IT IS well known that the infrared search and tracking (IRST) system has found wide applications in space surveillance, remote sensing, object tracking, and so on. Infrared small target detection plays a crucial role in the performances of IRST systems [1]. Due to the long imaging distance, the target is of small size without concrete shape and texture. Furthermore, the target is usually buried in the complex background and heavy noise, which causes its signal-to-noise ratio (SNR) to be quite low. Consequently, robust infrared small target detection is considered an extremely challenging problem. Although researchers have made extensive efforts on this task in the past decades [2], it still remains an open issue.

Recently, numerous methods have been proposed to solve this problem. Some conventional baseline methods have been used for infrared small target detection, such as median filter, top-hat filtering (THT) [3], and max-mean (MMEN) filter [4]. These methods attempt to estimate the image background and extract targets from the predicted background. However, they are sensitive to noise and not suitable for those backgrounds whose statistic characters are quickly varying. Motivated by recent advances in the robust principal component analysis (RPCA) [5], some methods were presented to detect infrared small target [6]. These methods assume that the background and the target components can be approximately represented by a low-rank matrix and a sparse matrix, respectively. Moreover, there exist other methods based on components analysis such as singular value decomposition [7] and partial sum minimization of singular values [8]. However, the process of RPCA is computationally expensive and time-consuming. In addition, some local contrast and human visual system (HVS)-based methods have attracted much attention, for instance, the methods based on multiscale patch-based contrast measure (MPCM) [9] and multiscale relative local contrast measure (MRLCM) [10]. Similarly, these methods perform poorly in either enhancement performance or detection accuracy when the targets are buried in intricate clutters.

In this letter, we propose an efficient and effective small target detection method for small targets embedded in diverse scenes. Note that the structure of the target region is dissimilar to the structures of the neighboring regions [11] and the size of the target may vary due to different target types, imaging distances, and environments. Therefore, we conceive a local dissimilarity descriptor encoded by the local energy factor (LEF). Then, an infrared small target detection method based on multiscale local contrast measure using LEF (MLCM-LEF) is designed.

II. Methodology

In this section, we first introduce the mathematical representation of the proposed local dissimilarity measure LEF. Next, we provide a description of the proposed small target detection method based on MLCM-LEF and present an explicit algorithm for it. Finally, we introduce the full framework of the proposed method.

A. Local Dissimilarity Measure Using LEF

1) Mathematical Representation of LEF: Assume that a normalized infrared image $\boldsymbol{f}$ with size of $m \times n$ is defined on the patch domain $\boldsymbol{F} \subset \mathbb{R}^2$. As shown in Fig. 1, we further assume that a local image patch $\boldsymbol{g}_{ij}$ with size of $3p \times 3p$ centered at an given pixel point (i, j) in $\boldsymbol{f}$ and another image patch $\boldsymbol{h}_{ij}$ with size of $p \times p$ are defined on the patch domain

Manuscript received November 18, 2018; revised April 11, 2019; accepted April 29, 2019. This work was supported in part by the National Nature Science Foundation of China under Grant 61671408, in part by the Shanghai Aerospace Science and Technology Innovation Fund under Grant SAST2015033, and in part by the Joint Fund of the Ministry of Education of China under Grants 6141A02022350 and 6141A02022362. *(Corresponding author: Xiaorun Li.)*

C. Xia and X. Li are with the College of Electrical Engineering, Zhejiang University, Hangzhou 310027, China (e-mail: auto_xia@foxmail.com; lxrly@zju.edu.cn).

L. Zhao is with the Institute of Computer Application Technology, Hangzhou Dianzi University, Hangzhou 310018, China (e-mail: zhaoly@hdu.edu.cn).

R. Shu is with the Shanghai Institute of Satellite Engineering, Shanghai 200240, China.

Color versions of one or more of the figures in this letter are available online at http://ieeexplore.ieee.org.

Digital Object Identifier 10.1109/LGRS.2019.2914432

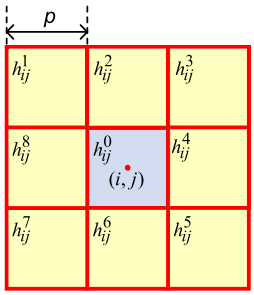

Fig. 1. Nested structure of a local image patch $\boldsymbol{g}_{ij}$.

$\boldsymbol{G}$ and $\boldsymbol{H}$ in $\mathbb{R}^2$, respectively. Also, we have $\boldsymbol{H} \subset \boldsymbol{G}$. The local image patch $\boldsymbol{g}_{ij}$ can be divided into nine subpatches $\boldsymbol{h}_{ij}^k \in \boldsymbol{H}$, $k = 0, 1, \ldots, 8$. To determine if the given pixel point (i, j) is a target (or part of a target), we must measure the dissimilarity between the central subpatch $\boldsymbol{h}_{ij}^0$ and the other subpatches. We first vectorize the subpatches $\boldsymbol{h}_{ij}^k$ along the column as columns x_{ij}^k of a 2-D matrix $\boldsymbol{X}_{ij}$, where $\boldsymbol{X}_{ij} = [x_{ij}^0, \ldots, x_{ij}^8]$. As discussed previously, only the relative brightness can generate light stimulus for HVS. Therefore, we reasonably quantify the light stimulus of $\boldsymbol{X}_{ij}$ by using centralized local energy E_{ij}, which is defined as follows:

$$E_{ij} = \|\boldsymbol{X}_{ij} - \overline{\boldsymbol{X}}_{ij}\|_F^2 \tag{1}$$

where $\|\cdot\|_F$ is the Frobenius norm (i.e., $\|A\|_F = (tr(A^T A))^{1/2} = (\sum_{pq} A_{pq}^2)^{1/2}$) and each column of $\overline{\boldsymbol{X}}_{ij}$ is the mean column vector of $\boldsymbol{X}_{ij}$.

Let $A = [a_1, \ldots, a_{i-1}, a_i, a_{i+1}, \ldots, a_n]$ be partitioned according to its columns, where $i = 1, \ldots, n$. Define

$$\mathrm{Del}(A, i) = [a_1, \ldots, a_{i-1}, a_{i+1}, \ldots, a_n] \tag{2}$$

that is, $\mathrm{Del}(A, i)$ denotes the matrix whose ith column is eliminated from A and whose remaining columns coincide with those of A. Consider a new matrix $\boldsymbol{X}_{ij}^{\neg 0} = Del(\boldsymbol{X}_{ij}, 1)$ that removes x_{ij}^0 from $\boldsymbol{X}_{ij}$, its centralized local energy can be obtained by

$$E_{ij}^{\neg 0} = \left\|\boldsymbol{X}_{ij}^{\neg 0} - \overline{\boldsymbol{X}}_{ij}^{\neg 0}\right\|_F^2 \tag{3}$$

where each column of $\overline{\boldsymbol{X}}_{ij}^{\neg 0}$ is the mean column vector of $\boldsymbol{X}_{ij}^{\neg 0}$.

Then, for any pixel point (i, j) in the normalized image $\boldsymbol{f}$, the proposed LEF is defined by

$$\begin{aligned} s_{ij} &= \frac{E_{ij}/\mathrm{Col}(\boldsymbol{X}_{\mathrm{ij}}) - \mathrm{E}_{\mathrm{ij}}^{\neg 0}/\mathrm{Col}\left(\boldsymbol{X}_{\mathrm{ij}}^{\neg 0}\right)}{E_{ij}/\mathrm{Col}(\boldsymbol{X}_{\mathrm{ij}})} \\ &= 1 - \frac{\mathrm{Col}(\boldsymbol{X}_{\mathrm{ij}})\mathrm{E}_{\mathrm{ij}}^{\neg 0}}{\mathrm{Col}\left(\boldsymbol{X}_{\mathrm{ij}}^{\neg 0}\right)\mathrm{E}_{\mathrm{ij}}} \end{aligned} \tag{4}$$

where $\mathrm{Col}(\boldsymbol{X})$ denotes the number of columns of $\boldsymbol{X}$. Namely, the LEF s_{ij} measures the local energy contribution that the subpatch $\boldsymbol{h}_{ij}^0$ centered at (i, j) makes to the local image patch $\boldsymbol{g}_{ij}$, that is, the local dissimilarity between $\boldsymbol{h}_{ij}^0$ and the remaining subpatches in $\boldsymbol{g}_{ij}$. In summary, the method to compute the LEF is given in Algorithm 1.

Algorithm 1 Computing LEF

Input: Local image patch $\boldsymbol{g}$ for an given pixel point.
Output: The LEF s.
1: Divide $\boldsymbol{g}$ into 9 sub-patches $\boldsymbol{h}^k$ $(k = 0, \ldots, 8)$.
2: Compute the centralized local energy E of $\boldsymbol{g}$ according to (1).
3: Remove $\boldsymbol{h}^0$ from $\boldsymbol{g}$ and update its centralized local energy $E^{\neg 0}$ according to (3).
4: Compute the LEF according to (4).

B. Multiscale Local Contrast Measure Using LEF

Generally, the discontinuity of a small target is described in two aspects: dissimilarity and brightness difference. Since we have measured the dissimilarity by LEF, we now consider conceiving a local contrast measure by taking both the dissimilarity and the brightness difference feature into account.

As depicted in Fig. 1, the gray mean of the surrounding subpatches (i.e., $\boldsymbol{h}_{ij}^k, k = 1, \ldots, 8$) at scale p is denoted by

$$m_{ij}^p = \frac{1}{8p^2} \sum_{k=1}^{8} \sum_{y=1}^{p} \sum_{x=1}^{p} h_{ij}^k(x, y). \tag{5}$$

Then, the local brightness difference measure at scale p for a given pixel point (i, j) in $\boldsymbol{f}$ is given by

$$d_{ij}^p = \alpha\left(f(i, j) - m_{ij}^p\right) \tag{6}$$

where $f(i, j)$ is the gray level of the pixel point (i, j) and α is a parameter determined as follows: if there are only bright targets (or dark targets) in a known application scenario, set α to 1 (or -1), if both types of targets are waiting to be detected, then set α to η_{ij}, where η_{ij} is computed by

$$\eta_{ij} = \begin{cases} 1 & \text{if } \mathrm{norm}\left(\overline{x}_{ij}^{\neg 0}\right) - \mathrm{norm}\left(\overline{x}_{ij}\right) > 0 \\ -1 & \text{if } \mathrm{norm}\left(\overline{x}_{ij}^{\neg 0}\right) - \mathrm{norm}\left(\overline{x}_{ij}\right) < 0 \end{cases} \tag{7}$$

where $\overline{x}_{ij}^{\neg 0}$ and $\overline{x}_{ij}$ denote the mean column vector of $\overline{\boldsymbol{X}}_{ij}^{\neg 0}$ and $\overline{\boldsymbol{X}}_{ij}$, respectively. It indicates that the target is a bright one if $\eta_{ij} = 1$, while a dark one if $\eta_{ij} = -1$.

For any given scale $p \in \{1, 3, \ldots, p_{\max}\}$, the LEF map denoted by $\boldsymbol{s}^p$ and the local brightness difference map denoted by $\boldsymbol{d}^p$ are achieved by making each of them traverse the image patch at scale p, respectively. Next, we normalize both $\boldsymbol{s}^p$ and $\boldsymbol{d}^p$ at all scales ($p = 1, 3, \ldots, p_{\max}$) to the range [0, 1], which are given by

$$\tilde{s}^p(i, j) = (s^p(i, j) - s_{\min})/(s_{\max} - s_{\min}) \tag{8}$$

$$\tilde{d}^p(i, j) = (d^p(i, j) - d_{\min})/(d_{\max} - d_{\min}) \tag{9}$$

where $s_{\min}$ and $s_{\max}$ are the minimum and the maximum of the LEF maps at all scales, respectively. Similarly, $d_{\min}$ and $d_{\max}$ denote the minimum and the maximum of the local brightness difference maps at all scales, respectively. Then, we conceive a confidence measure to robustly represent the local contrast, which is computed as the product of a weighted 2-D Gaussian kernel centered at (1, 1) [12]

$$G(x, y) = \exp\left\{\frac{\alpha(\mathrm{x} - 1)^2 + (1 - \alpha)(\mathrm{y} - 1)^2}{-2\mathrm{h}^2}\right\} \tag{10}$$

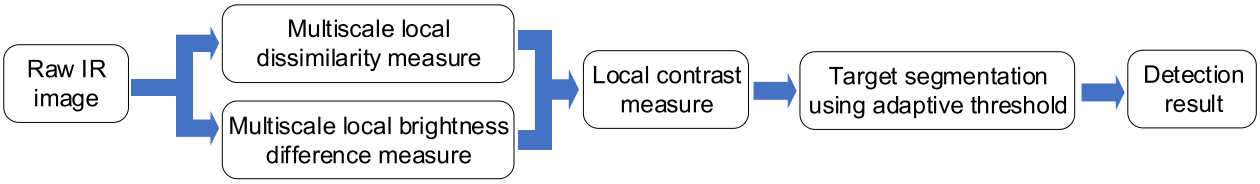

Fig. 2. Flowchart of the proposed small target detection method.

Algorithm 2 Computing an MLCM-LEF Map

Input: Given an input image $\boldsymbol{f}$.
Output: The MLCM-LEF map $\boldsymbol{c}$.

for p=1:2:$p_{\max}$ **do**
  for i=1:m **do**
    for j=1:n **do**
      $s^p(i,j)$ is computed according to Algorithm 1.
      $d^p(i,j)$ is computed by (6).
    end for
  end for
end for
$\tilde{s}^p$ is obtained by normalizing s^p according to (8).
$\tilde{d}^p$ is obtained by normalizing d^p according to (9).
for i=1:m **do**
  for j=1:n **do**
    $c(i,j)$ is computed by (11).
  end for
end for

where h and α are the constants that control the denoising effect and the influence of input parameters, respectively. These two constants will be discussed in Section III-A. As mentioned previously, the size of the target usually cannot be determined beforehand. However, in order to obtain the valid local contrast measure, the local patch size determined by p in (8) and (9) should be approximated to the size of the target. In this case, the theory of multiscale analysis is utilized. Let $\boldsymbol{c}$ denote an MLCM-LEF map defined on an image patch domain $\boldsymbol{C}$ and a mapping $\psi : \boldsymbol{F} \to \boldsymbol{C}$ is defined as follows: given a pixel point (i,j) in $\boldsymbol{f} \in \boldsymbol{F}$, its MLCM-LEF value is given by substituting $\tilde{s}^p(i,j)$ and $\tilde{d}^p(i,j)$ into (10), that is,

$$c(i,j) = \psi\left(f(i,j)\right) = \max_{p=1,3,\ldots,p_{\max}} G(\tilde{s}^p(i,j), \tilde{d}^p(i,j)). \tag{11}$$

The concrete computation process of the MLCM-LEF map is presented in Algorithm 2, where m and n denote the size of $\boldsymbol{f}$.

C. Small Target Detection Based on MLCM-LEF

The contrast between a small and dim target and its background is greatly enlarged by using the proposed local contrast measure. Therefore, it is much easier to detect the target in the MLCM-LEF map. In this letter, we segment the target by using an adaptive threshold denoted by

$$\tau = \mu + K\sigma \tag{12}$$

where μ and σ are the mean value and the standard deviation of the MLCM-LEF map, respectively, and K is an empirical constant. Our experiments suggest that the optimal range of K is [5, 25]. Based on the aforementioned preparation, a small target detection method is designed. Fig. 2 shows the flowchart of the proposed small target detection approach.

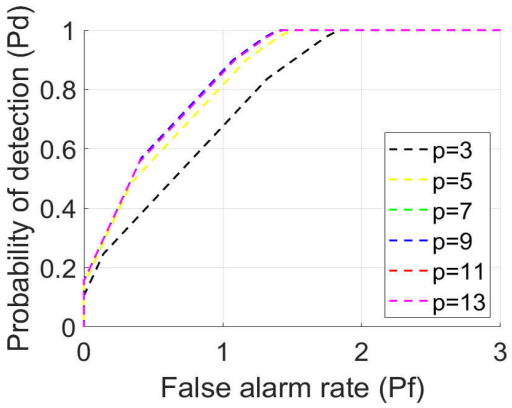

Fig. 3. ROC curves of Sequence 2 for different $p_{\max}$.

III. Experimental Results

In this section, we first provide detailed discussions of the parameters involved in our method. Then, a comprehensive comparison of all the methods is presented to demonstrate the effectiveness and robustness of our method. In the experiments, the signal-to-clutter ratio gain (SCRG) and the background suppression factor (BSF) are adopted as a performance indicator for target enhancement and detection [7]. Also, the receiver operating characteristic (ROC) curves [2] are used to evaluate the detection performance of target detection methods. A test data set containing three real consecutive sequences and a single-frame image set is used and its detailed information is listed in Table I. Particularly, Sequence R contains representative infrared images with small targets embedded in diverse backgrounds, e.g., cars on the country roads, ships at sea, and so on. All experiments are implemented using MATLAB R2018a on a computer with a 3.6-GHz Intel core i7 CPU and 8 GB RAM.

A. Sensitivity Analysis of the Crucial Parameters

There are only three parameters involved in the proposed method, that is, the global smoothing parameter h, the weight parameter α in (10), and the maximal scale $p_{\max}$ in (11). Note that h controls the denoising effect and only relates to enhancement performance. We find the targets are well enhanced when h is set from 0.2 to 1. Hence, we set $h = 0.2$ in the following experiments. The weight parameter α is used for controlling the influence degree of LEF $\tilde{s}^p(i,j)$ and local

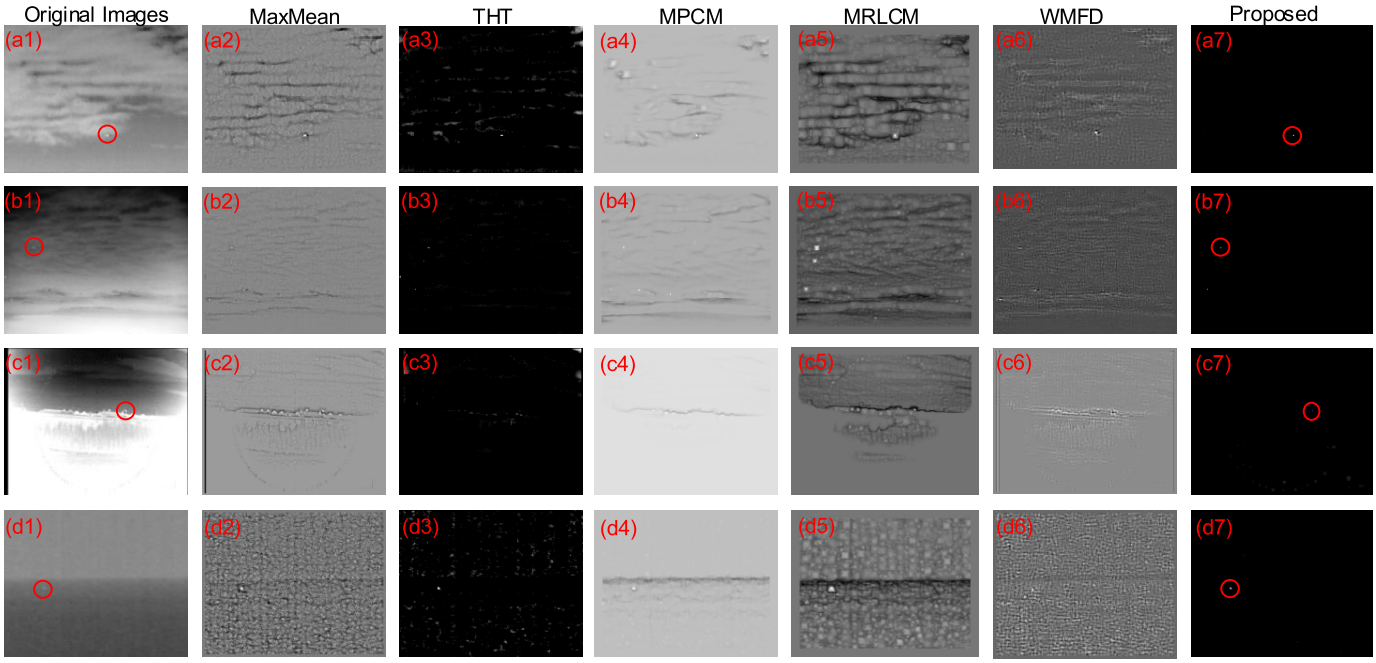

Fig. 4. Enhancement results of various methods testing on the representative frames in the sequences. (a1)–(d1) Selected from Sequences 1, 2, 3, and R, respectively. Red circles: where the targets appear.

TABLE I
INFORMATION OF THE TEST DATA SET

	#Frames	#Targets	Frame Size	Target Category	Target Size	Background Type	Image quality
Sequence 1	30	44	256×200	Airplane	6×4	Heavy cloudy	Heavy noise
Sequence 2	300	300	320×250	Airplane	5×3 to 5×7	Sky	Many dead pixels
Sequence 3	100	100	320×240	Bird	4×4 to 9×7	Sky-gound	Overexposure and dark margins
Sequence R	26	31	125×125	Cars, ships, etc.	3×3 to 9×7	Sea, road, etc.	Complex exposure conditions

brightness difference measure $\tilde{d}^p(i, j)$ in (11). Experimental results suggest that our model is not sensitive to α, and choosing α from the interval $[0.2, 0.8]$ can provide satisfactory detection performance. In the following experiments, we set α to 0.5. The parameter $p_{\max}$ is associated with the maximal potential size of small targets. According to the definition of Society of Photo-Optical Instrumentation Engineers, a small target has a total spatial extent of less than 80 pixels [13]. Consequently, we appropriately set $p_{\max} = 9$ to constrain the target size to $9 \times 9 = 81$ pixels. To verify it, we test different $p_{\max}$ on Sequence 2 using our method, and the ROC curves are displayed in Fig. 3. We can see in Fig. 3 that setting $p_{\max}$ to 9 performs the best.

B. Comprehensive Comparison

1) Enhancement Performance: To demonstrate the superiority of the proposed method, several state-of-the-art methods based on MMEN [4], THT [3], MPCM [9], MRLCM [10], and gradient direction diversity-weighted multiscale flux density (WMFD) [2] are used for comparison. Sample visual results of different methods are shown in Fig. 4. It can be seen in Fig. 4 that our method can robustly eliminate more clutters and noise, compared with the baseline methods. In addition, quantitative comparisons are summarized in Table II. We can see in Table II that the proposed method noticeably outperforms the baseline methods in both SCRG and BSF. Therefore, we can draw a conclusion that our method does better in enhancing small and dim target and suppressing intricate background simultaneously.

2) Detection Performance: Fig. 5 displays the ROC curves obtained by testing all the methods on the data set. The candidate targets detected by different methods are considered correct if their pixel distances to the center of the ground truth of the targets are less than 3 pixels. As depicted in Fig. 5, our method has better detection performance compared with the baseline methods. From the results of the above-mentioned experiments, it can be found that the proposed method achieves the best detection performance and works robustly and effectively for small and dim targets detection under different backgrounds and heavy noise.

3) Computational Complexity: The average running time of all the methods is given in Table II, in which we can see that the proposed algorithm is not time-consuming and its theoretically computational complexity is around $O(mnp_{\max}^3)$.

TABLE II
AVERAGE EVALUATION VALUE OF DIFFERENT METHODS FOR THE DATA SET

		MMEN in [4]	THT in [3]	MPCM in [9]	MRLCM in [10]	WMFD in [2]	Ours MLCM-LEF
Sequence 1	$\overline{SCRG}$	0.8261	3.5101	1.9428	1.1706	1.3122	**5.6226**
	$\overline{BSF}$	2.4143	4.0456	3.5883	2.1492	3.4350	**9.4332**
	$\overline{Time}$ (s)	0.3765	0.6474	3.3479	8.2427	2.7777	5.6703
Sequence 2	$\overline{SCRG}$	0.5433	2.3251	2.5112	0.9640	0.7507	**14.2222**
	$\overline{BSF}$	10.5299	7.3354	19.2082	5.7079	6.7750	**49.1659**
	$\overline{Time}$ (s)	0.5572	0.0303	5.2819	13.4735	4.4714	9.6553
Sequence 3	$\overline{SCRG}$	0.7005	4.8759	1.7931	1.0079	0.6808	**493.6450**
	$\overline{BSF}$	7.1960	25.5728	12.4371	1.4135	9.6930	**58.9602**
	$\overline{Time}$ (s)	0.6286	0.0313	7.6518	12.0399	4.1875	8.7768
Sequence R	$\overline{SCRG}$	0.8316	11.1578	2.9699	1.1260	0.7572	**1808.533**
	$\overline{BSF}$	4.0224	5.1196	6.0885	3.8894	4.7243	**17.4876**
	$\overline{Time}$ (s)	0.1666	0.0442	1.6208	2.7644	1.0004	2.0097

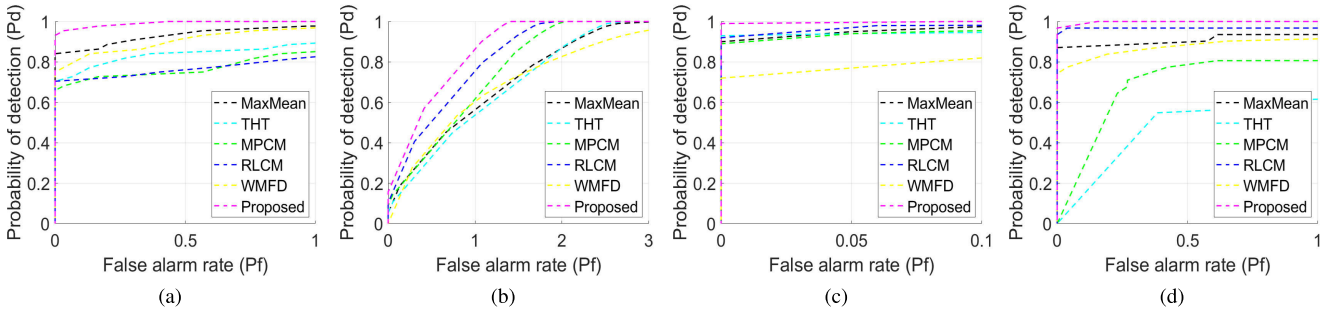

Fig. 5. ROC curves of the proposed method and the baseline methods for three real IR sequences and Sequence R. (a) Result of Sequence 1. (b) Result of Sequence 2. (c) Result of Sequence 3. (d) Result of Sequence R.

IV. CONCLUSION

A small target detection method based on MLCM-LEF is presented in this letter. Extensive real data experiments have verified that the proposed method is effective and robust to detect small and dim targets in infrared images with poor quality. Our future interest is applying LEF to spectral dissimilarity measure in 3-D images, for example, multispectral images and hyperspectral images. In addition, we note that the proposed method can be easily accelerated by a GPU or field-programmable gate array (FPGA).

REFERENCES

[1] C. L. P. Chen, H. Li, Y. Wei, T. Xia, and Y. Y. Tang, "A local contrast method for small infrared target detection," *IEEE Trans. Geosci. Remote Sens.*, vol. 52, no. 1, pp. 574–581, Jan. 2014.

[2] D. Liu, L. Cao, Z. Li, T. Liu, and P. Che, "Infrared small target detection based on flux density and direction diversity in gradient vector field," *IEEE J. Sel. Topics Appl. Earth Observ. Remote Sens.*, vol. 11, no. 7, pp. 2528–2554, Jul. 2018.

[3] X. Bai and F. Zhou, "Analysis of new top-hat transformation and the application for infrared dim small target detection," *Pattern Recognit.*, vol. 43, no. 6, pp. 2145–2156, 2010. [Online]. Available: http://www.sciencedirect.com/science/article/pii/S0031320310000105

[4] S. D. Deshpande, M. H. Er, R. Venkateswarlu, and P. Chan, "Max-mean and max-median filters for detection of small targets," *Proc. SPIE*, vol. 3809, pp. 74–84, Oct. 1999. doi: 10.1117/12.364049.

[5] E. J. Candès, X. Li, Y. Ma, and J. Wright, "Robust principal component analysis?" *J. ACM*, vol. 58, no. 3, p. 11, May 2011. doi: 10.1145/1970392.1970395.

[6] C. Q. Gao, D. Meng, Y. Yang, Y. Wang, X. Zhou, and A. G. Hauptmann, "Infrared patch-image model for small target detection in a single image," *IEEE Trans. Image Process.*, vol. 22, no. 12, pp. 4996–5009, Dec. 2013.

[7] Y. Li *et al.*, "An infrared target detection algorithm based on lateral inhibition and singular value decomposition," *Infr. Phys. Technol.*, vol. 85, pp. 238–245, Sep. 2017. [Online]. Available: http://www.sciencedirect.com/science/article/pii/S1350449517301500

[8] Y. Dai, Y. Wu, Y. Song, and J. Guo, "Non-negative infrared patch-image model: Robust target-background separation via partial sum minimization of singular values," *Infr. Phys. Technol.*, vol. 81, pp. 182–194, Mar. 2017. [Online]. Available: http://www.sciencedirect.com/science/article/pii/S1350449516303723

[9] Y. Wei, X. You, and H. Li, "Multiscale patch-based contrast measure for small infrared target detection," *Pattern Recognit.*, vol. 58, pp. 216–226, Oct. 2016. [Online]. Available: http://www.sciencedirect.com/science/article/pii/S0031320316300358

[10] J. Han, K. Liang, B. Zhou, X. Zhu, J. Zhao, and L. Zhao, "Infrared small target detection utilizing the multiscale relative local contrast measure," *IEEE Geosci. Remote Sens. Lett.*, vol. 15, no. 4, pp. 612–616, Apr. 2018.

[11] J. F. Khan and M. S. Alam, "Target detection in cluttered forward-looking infrared imagery," *Opt. Eng.*, vol. 44, no. 7, Jul. 2005, Art. no. 076404.

[12] L. M. J. Florack, B. M. Ter Haar Romeny, J. J. Koenderink, and M. A. Viergever, "Linear scale-space," *J. Math. Imag. Vis.*, vol. 4, no. 4, pp. 325–351, Dec. 1994. doi: 10.1007/BF01262401.

[13] W. Zhang, M. Cong, and L. Wang, "Algorithms for optical weak small targets detection and tracking: Review," in *Proc. Int. Conf. Neural Netw. Signal Process.*, Dec. 2003, pp. 643–647.